





Research Article

Assessment of Real-Time Compaction Quality Test Indexes for Rockfill Material Based on Roller Vibratory Acceleration Analysis

Tianbo Hua ^{1,2}, Xingguo Yang ^{1,2}, Qiang Yao ^{1,2} and Hongtao Li ^{1,2}

¹State Key Laboratory of Hydraulics and Mountain River Engineering, Sichuan University, Chengdu, Sichuan 610065, China

²College of Water Resource and Hydropower, Sichuan University, Chengdu, Sichuan 610065, China

Correspondence should be addressed to Hongtao Li; htl@scu.edu.cn

Received 25 September 2017; Revised 8 November 2017; Accepted 21 November 2017; Published 20 February 2018

Academic Editor: Antonio Gilson Barbosa de Lima

Copyright © 2018 Tianbo Hua et al. This is an open access article distributed under the Creative Commons Attribution License, which permits unrestricted use, distribution, and reproduction in any medium, provided the original work is properly cited.

Compaction quality is directly related to the structure and seepage stability of a rockfill dam. To timely and accurately test the compaction quality of the rockfill material, four real-time test indexes were chosen to characterize the soil compaction degree based on the analysis of roller vibratory acceleration, including acceleration peak value (a_p), acceleration root mean square value (a_{rms}), crest factor value (CF), and compaction meter value (CMV). To determine which of these indexes is the most appropriate, a two-part field compaction experiment was conducted using a vibratory roller in different filling zones of the dam body. Data on rolling parameters, real-time test indexes, and compaction quality indexes were collected to perform statistical regression analyses. Combined with the spectrum analysis of the acceleration signal, it was found that the CF index best characterizes the compaction degree of the rockfill material among the four indexes. Furthermore, the quantitative relations between the real-time index and compaction quality index were established to determine the control criterion of CF, which can instruct the site work of compaction quality control in the rockfill rolling process.

1. Introduction

The layered filling compaction of dam materials is an important process in the construction of a rockfill dam. An effective compaction quality control is the key to ensure the safe and stable operation of the dam. Nowadays, the compaction quality control in rockfill dam projects mainly depends on the manual control of rolling parameters and random spot tests after construction, which is normally called the “dual control method” [1]. With the expansion of the filling scale, this traditional compaction quality control method has been unable to meet the requirements of modern mechanized construction. Therefore, it has been quite necessary to develop a fast, real-time, and accurate compaction quality test method with continuous, automatic, and high precision characteristics.

To provide a quality-inspection process that is more reliable and timely, previous studies in the field of transportation engineering focused on correlating compaction quality to soil properties and construction-operating parameters that can be obtained easily and quickly from the

field. Geodynamik and Dynapac of Sweden characterized compaction quality by compaction meter value (CMV), which is the ratio between the amplitude of the first harmonic and that of the fundamental frequency [2, 3]. Previous studies verified that CMV is closely related to the fundamental reaction and physical properties of the compacted soil [4–7]. According to Forssblad [8–11], CMV has been noted to range from 40 to 70 for gravel, from 25 to 40 for sand, and from 20 to 30 for silt.

The compaction control value (CCV) adopted by Sakai company is similar to CMV, which is also determined from the measured acceleration data but based on more harmonic frequency components, including 0.5, 1, 1.5, 2, 2.5, and 3 fundamental frequency and harmonic components [12, 13]. Caterpillar used machine drive power (MDP) to determine the compaction characteristics in road work [14, 15], which originated from the study of vehicle-terrain interaction [16]. Researchers found that MDP is highly correlated with compaction density and elastic modulus of the soil [17–19].

Bomag from Germany used a software algorithm which derived from a mechanical model to calculate the dynamic

modulus E_{vib} of the material to describe the compacted condition of soil [20]. Mooney and Rinehart [21] and Rinehart and Mooney [22] proposed that the total harmonic distortion (THD) is a highly sensitivity index to evaluate the soil compaction state. The larger the THD, the stiffer the soil will be. Ammann calculated the soil stiffness, K_B , as a measure of compaction quality [23] and verified the strong correlation between K_B and soil rigidity [24, 25]. China Southwest Jiaotong University used vibratory compaction value (VCV), a dynamic subgrade structural reaction index, to evaluate the soil compaction quality and achieved good results in a roadbed continuous compaction quality test [26].

However, the abovementioned researches are mainly carried out on the subgrade filling material. In fact, there are great differences between the rockfill in earth-rock dams and the subgrade filler in road engineering in terms of the soil particle size and shape. At present, the maximum particle size of the rockfill in hydropower projects has reached 1 m, and many particles are solid block stones with sharp and jagged edges. In contrast, the maximum particle size of the subgrade filler is generally less than often 150 mm, and the main contents are spherical particles with few edges [13]. This makes the compaction characteristics of the two materials quite different. Therefore, further study is needed to know whether the index that applied well on subgrade filler can also achieve excellent test results on the rockfill material of earth-rock dams.

The objective of this study is to obtain an index that can characterize the compaction degree of the rockfill material timely and accurately. The rockfill material tested in the experiment belongs to cohesionless coarse-grained soil; therefore, the compaction degree in the study actually refers to the physical indicator of relative density. The following section first analyzes the relationship between the roller vibratory acceleration and the soil compaction degree. Then, combined with the abovementioned study, four real-time test indexes derived from acceleration signal were chosen to characterize the rockfill compaction degree. To analyze and judge the detection effect of each index on the rockfill material, comparison experiments were conducted in different filling zones of the dam body with different rolling parameters. Statistical regression analysis of test data and spectrum analysis of acceleration signal were then performed to get the final conclusions.

2. Methodology

This section first introduces the terrain-vehicle dynamical model in the existing literature and analyzes the relationship between roller vibratory acceleration and the compacted condition of soil. Next, the four real-time test indexes utilized in the experimental test are introduced, with their calculating methods and physical significances elaborated. Finally, the testing method and equipment are presented.

2.1. Vibration Model. According to the study of terrain-vehicle systems [16] and the research on the vibratory roller from Yoo and Selig [27–29], it can be known that the acceleration of the vibratory roller is closely related to the

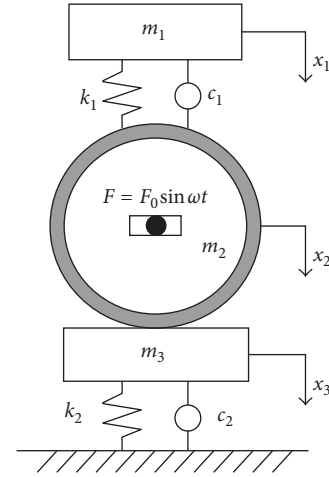


FIGURE 1: Terrain-vehicle dynamical model. m_1 : frame mass, m_2 : roller mass, m_3 : soil mass, k_1 : roller-frame stiffness, c_1 : roller-frame damping, k_2 : soil stiffness, c_2 : soil damping, x_1 : vertical displacement of frame, x_2 : vertical displacement of roller, x_3 : vertical displacement of soil, F : excitation force, \ddot{x} : acceleration.

compaction condition of the pressed material. The terrain-vehicle vibration model [29] can be described as in Figure 1.

To facilitate the calculation and analysis, the model is simplified by not taking the horizontal displacement and jump vibration of the vibratory roller into account. In such case, m_2 and m_3 always remain in contact, that is, $x_2 = x_3$. The force equations between the layers are expressed as

$$\begin{aligned} m_1 \ddot{x}_1 + c_1 (\dot{x}_1 - \dot{x}_2) + k_1 (x_1 - x_2) &= 0, \\ (m_2 + m_3) \ddot{x}_2 + (c_1 + c_2) \dot{x}_2 + (k_1 + k_2) x_2 & \\ - c_1 \dot{x}_1 - k_1 x_1 &= F_0 \sin \omega t. \end{aligned} \quad (1)$$

The equations can be expressed into matrix form as

$$\begin{bmatrix} m_1 & 0 \\ 0 & m_2 + m_3 \end{bmatrix} \begin{bmatrix} \ddot{x}_1 \\ \ddot{x}_2 \end{bmatrix} + \begin{bmatrix} c_1 & -c_2 \\ -c_1 & c_1 + c_2 \end{bmatrix} \begin{bmatrix} \dot{x}_1 \\ \dot{x}_2 \end{bmatrix} + \begin{bmatrix} k_1 & -k_2 \\ -k_1 & k_1 + k_2 \end{bmatrix} \begin{bmatrix} x_1 \\ x_2 \end{bmatrix} = \begin{bmatrix} 0 \\ F_0 \sin \omega t \end{bmatrix}. \quad (2)$$

By analytic calculation, we can obtain

$$|\ddot{x}_2| = \omega^2 |x_2| = \omega^2 F_0 \left(\frac{A_1^2 + B_1^2}{C^2 + D^2} \right)^{1/2} = f(k_2, c_2), \quad (3)$$

where $A_1 = k_1 - m_1 \omega^2$, $B_1 = c_1 \omega$, $C = (m_2 + m_3) m_1 \omega^4 - (m_2 + m_3) k_1 \omega^2 - m_1 k_2 \omega^2 - c_1 c_2 \omega^2 + k_1 k_2 - m_1 k_1 \omega^2$, and $D = k_2 c_1 \omega + k_1 c_2 \omega - (m_2 + m_3) c_1 \omega^3 - m_1 c_2 \omega^3 - m_1 c_1 \omega^3$.

It can be seen from (3) that the vertical vibratory acceleration of the roller (\ddot{x}_2) is related only to the stiffness k_2 and damping c_2 of the pressed soil. With the stiffness and damping of the soil directly reflecting the compactness of the soil, the roller vibratory acceleration (hereinafter referred to as a) and the soil compaction degree are closely related. However, due to the complexity of (3), the relationship between k_2 , c_2 , and a cannot be expressed with a definite function formula. The purpose of the experiment

is to gain a dataset of roller vibratory acceleration and soil compactness, then finding out the definite relationship between them.

2.2. Real-Time Test Indexes. The study of Zhong et al. [30, 31] and Liu et al. [32, 33] indicates that describing the soil compactness by directly using vibratory acceleration index a causes much uncertainty and volatility. Therefore, the following four derived indexes are selected by analyzing the roller acceleration signal.

2.2.1. Acceleration Peak Value (a_p). This index describes the amplitude variation of roller acceleration signal and is calculated as

$$a_p = \max\{|a_i|\} \quad (i = 1, 2, \dots, n), \quad (4)$$

where a_i is a random acceleration measurement and n is the number of collected samples within a certain period.

2.2.2. Acceleration Root Mean Square Value (a_{rms}). This index reflects the effective vibratory acceleration in the rolling process, which is calculated as

$$a_{\text{rms}} = \sqrt{\frac{1}{n} \sum_{i=1}^n a_i^2} = \sqrt{\frac{a_1^2 + a_2^2 + \dots + a_n^2}{n}}. \quad (5)$$

2.2.3. Crest Factor Value (CF). This index is a common evaluation index in alternating current, which is used to describe the ability of the AC power to output peak load current [34]. The CF value of a standard sinusoidal wave is 1.414. When the wave is distorted, the CF changes significantly. It is used by the authors to describe the waveform variation law of the roller vibratory acceleration signal and is defined as

$$\text{CF} = \frac{a_p}{a_{\text{rms}}}. \quad (6)$$

The formula shows that CF is a dimensionless acceleration index that integrates the variation trend of a_p and a_{rms} . The physical meaning of the index in this experiment is to describe the ability of the roller to output peak acceleration, namely, the ability of the soil to produce the greatest reaction force to the roller.

2.2.4. Compaction Meter Value (CMV). The index shows the ratio between the amplitude of the first harmonic and that of the fundamental frequency, which is obtained by the tuning analysis of the acceleration signal. The definition of CMV is expressed as

$$\text{CMV} = C \cdot \frac{A_1}{A_0}, \quad (7)$$

where C is the amplification coefficient and usually sets as 300, A_1 refers to the amplitude of the first harmonic of vibratory acceleration, and A_0 refers to the amplitude of the fundamental frequency of vibratory acceleration.

2.3. Testing Method. The experiment adopts the DHDAS dynamic signal acquisition system of Donghua (Figure 2), which mainly includes the acceleration sensor, the vibration data acquisition instrument, and the monitoring and analysis software for clients. The main physical quantity tested in the experiment is the vertical vibratory acceleration of the roller and its main vibration frequency. The roller used is the 32 t single-drum vibratory roller of Jointark mechanical YZ series (Figure 3). The sensors were installed vertically on the inner frame of the roller, and the data were collected simultaneously with the dual channel.

The a_p index is directly read by DHDAS software, and a_{rms} index is calculated by (5) with the tested acceleration data in a certain period. The CF is worked out by (6) with the measured a_p and a_{rms} . CMV is calculated by (7) with the amplitude of the first harmonic and that of the fundamental frequency in the spectrum of acceleration signal, which is obtained through fast Fourier transformation (FFT) analysis.

3. Experimental Testing

3.1. Testing Site and Materials. The experiment was carried out at the construction site of Chang-he Dam hydropower station, which located in Dadu River, China. The Chang-he Dam is a 240-meter-high core rockfill dam, and the structural design of it is shown in Figure 4. The experimental material includes the main rockfill, secondary rockfill, and filter material. Figure 5 shows the field experiment on the main rockfill, and the grain size distribution of the material is shown in Figure 6(a). The main compaction parameters of the test material are shown in Table 1.

In Table 1, the parameter “rolling times” means the compaction pass of the vibratory roller on each strip. The index relative density is defined as

$$D_r = \frac{e_{\text{max}} - e}{e_{\text{max}} - e_{\text{min}}} = \frac{(\rho_d - \rho_{d\text{min}})\rho_{d\text{max}}}{(\rho_{d\text{max}} - \rho_{d\text{min}})\rho_d}, \quad (8)$$

where e_{max} is the maximum void ratio, e_{min} is the minimum void ratio, e is the compacted void ratio, $\rho_{d\text{max}}$ refers to the maximum dry density, $\rho_{d\text{min}}$ refers to the minimum dry density, and ρ_d refers to the compacted dry density.

The index ρ_d is calculated by measuring the volume and dry weight of the soil sample collected from the field. The index $\rho_{d\text{max}}$ and $\rho_{d\text{min}}$ need to be measured in the laboratory individually. As the maximum particle size that can be tested by the device in the lab is 60 mm, the maximum grain size of the rockfill in the project has reached 800 mm. The oversize particles were replaced by the soil whose particle size is smaller than 60 mm and larger than 5 mm with equal mass, and at the ratio calculated by (9), which is called the equivalent weight replacement method [35]. The grading curve of the main rockfill after replacement is shown in Figure 6(b).

$$P_i = \frac{P_{oi}}{P_5 - P_{d\text{max}}} P_5, \quad (9)$$



FIGURE 2: DHDAS dynamic signal acquisition and analysis system. (a) Data acquisition instrument. (b) Data analysis system.



FIGURE 3: The vibratory roller and setting of sensors. (a) Vibratory roller. (b) Setting of sensors.

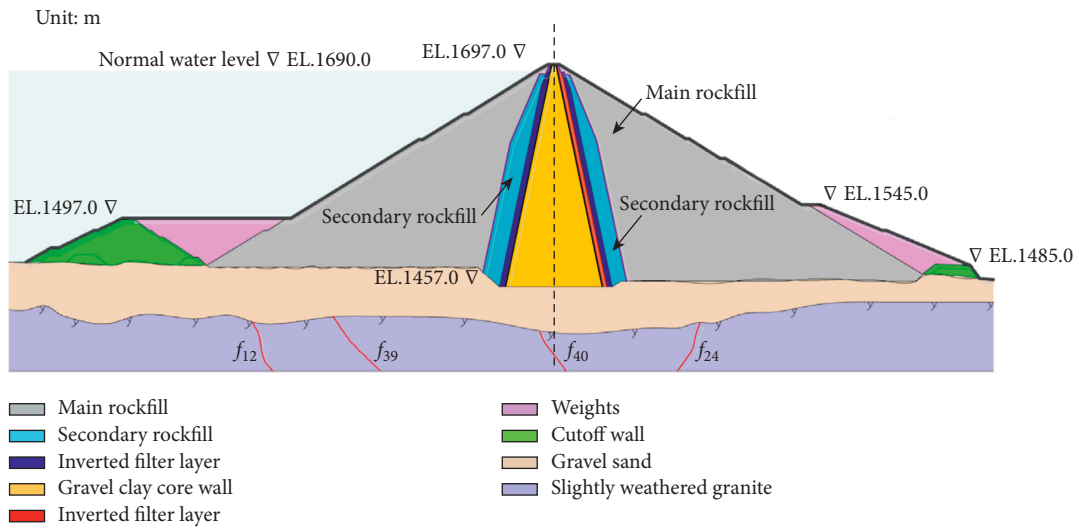


FIGURE 4: Structural diagram of Chang-he Dam.

where P_i refers to the weight percentage of some particle size group in the soil after replacement, P_{oi} refers to the weight percentage of some particle size group in the original soil, P_5 refers to the weight percentage of the soil whose particle size is larger than 5 mm, and P_{dmax} refers to the weight percentage of the oversize particles in the original soil.

After the replacement work to the soil sample, ρ_{dmin} and P_{dmax} can be calculated out with the volume and weight of the dried soil in the sample cylinder under the state of fluffy and the state after 8 min vibration on the platform vibrator respectively, which is called the loose filling test method and the platform vibrator experiment method [35], respectively.



FIGURE 5: Field experiment on the main rockfill. (a) Main rockfill. (b) Field experiment.

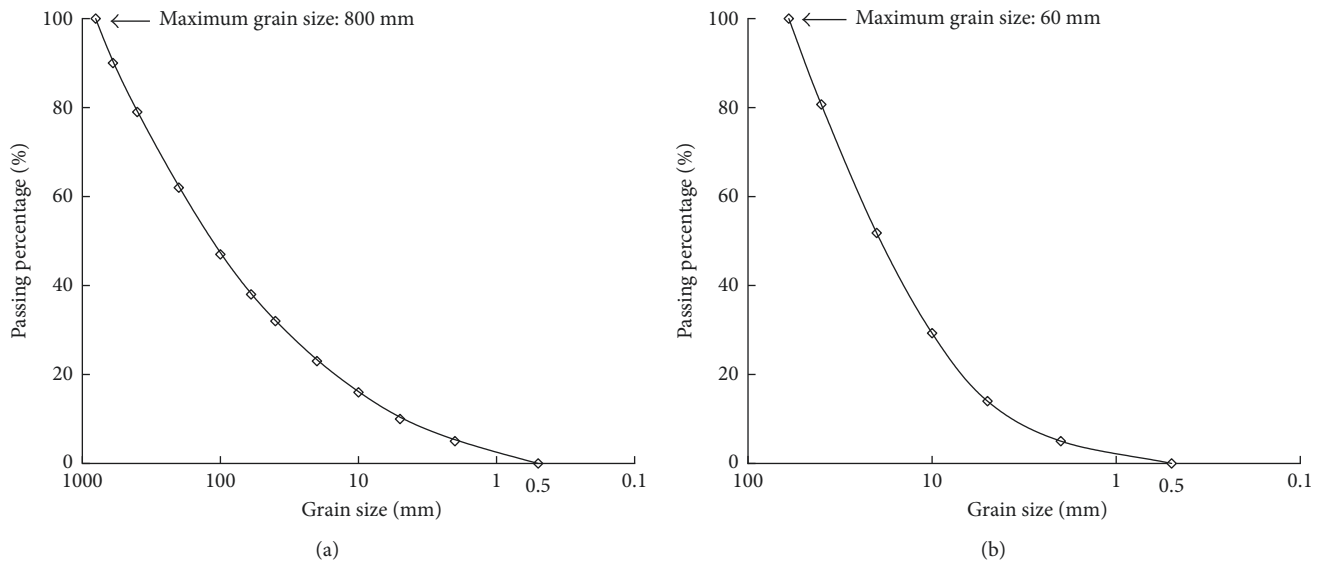


FIGURE 6: Grain size distribution of the main rockfill. (a) The original. (b) After replacement.

TABLE 1: Compaction parameters of the test material.

Testing material	Standard rolling parameters			Requirements of compaction quality indexes		
	Rolling times	Layer thickness (cm)	Driving speed (km/h)	Relative density	Dry density (g/cm^3)	Porosity
Main rockfill	Static roll (2), vibratory roll (8)	100	2.7 ± 0.2	—	≥ 2.22	$\leq 21\%$
Secondary rockfill	Static roll (2), vibratory roll (8)	50	2.7 ± 0.2	≥ 0.90	≥ 2.33	$\leq 20\%$
Filter material	Static roll (2), vibratory roll (8)	30	2.7 ± 0.2	≥ 0.85	≥ 2.08	—

3.2. Testing Program. To evaluate the test effects of indexes a_p , a_{rms} , CF, and CMV on rockfill and other dam materials comprehensively, a two-part field experiment was performed. Part 1 was used to evaluate the relationship between the four real-time test indexes and the rolling parameters. Part 2 was targeted at studying the correlation between real-time test indexes and compaction quality indexes. The results of experimental testing will provide a dataset for the subsequent modeling analysis in Section 4.

3.2.1. Experiment Part 1. Experiment part 1 was carried out with the rolling parameters of rolling times, running speed, and compaction thickness changed. Since the roller keeps in a vibration state of low frequency and high amplitude in the rolling process, the parameter of roller excitation force remains unchanged in the experiment.

For the cohesionless soil of the rockfill in the study, a high compacted dry density can be achieved under the condition of completely dry or fully saturated in the Proctor

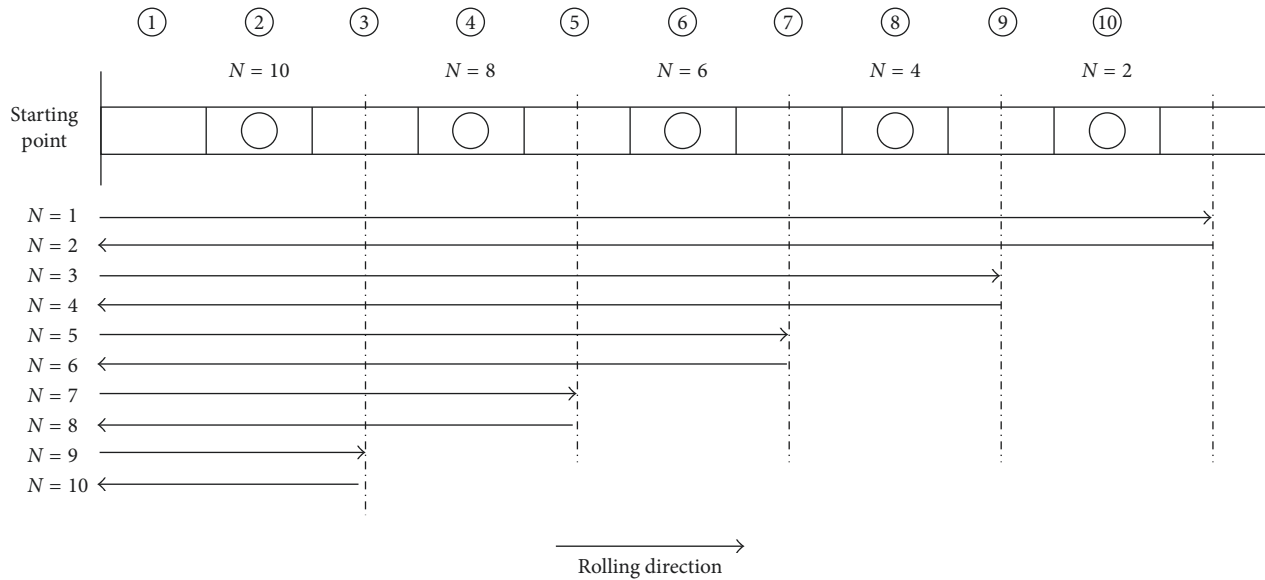


FIGURE 7: Rolling route of the vibratory roller (N : rolling times).

compaction test. However, due to the high hydraulic conductivity of the rockfill material, it is very hard for the material to keep high water content in the field compaction. And it is easy to raise dust if the dam material is completely dry, which is adverse to the construction environmental protection. Based on the comprehensive consideration of field compaction effect and construction cost and conditions, the water content of the rockfill material was kept at 1%–2% (weight ratio) in the field. The control method is to calculate and add water to the dam material automatically by using the intelligent water adding system developed by Sinohydro Bureau 5 Co., Ltd. before paving and supplement water to the paved soil with the sprinkling truck to maintain the water content before compaction.

Combined with the analysis above, the specific test plan can be made as follows by not taking the parameters of excitation force and water content into account.

- (1) Change in rolling times: one rolling strip was selected in the filling zone of each test material with a length of 60 m and width of 2.2 m (width of the roller), respectively. As the dam material in the rolling strip cannot be completely even in the paving process, the data measured in different regions of the same strip change greatly. Therefore, the test strips are divided into small test areas with the grid of 5 m long and 2.2 m wide (Figure 5(b)), and the data on each small test area are analyzed separately. The standard vibratory rolling times of the test material is eight times (Table 1). In order to increase the sample volume and observe the variation trend of acceleration signal when the compaction pass exceeds standard, the number of vibratory rolling times is set at ten times.
- (2) Change in running speed and compaction thickness: three adjacent strips were selected in the main and secondary rockfill zones, respectively, to analyze the change of each index brought by different running

speeds, where the vibratory roller proceeded with low speed ($v = 1.8$ km/h), medium speed ($v = 2.2$ km/h), and high speed ($v = 2.6$ km/h). The same goes to the number of test strips in the experiment of change in compaction thickness. The thickness of the test strip on main rockfill was set to be 80 cm, 100 cm, and 120 cm, respectively, and that of the secondary rockfill to be 30 cm, 60 cm, and 90 cm, respectively.

3.2.2. Experiment Part 2. To conduct the correlation test of real-time test index and compaction quality index, experiment part 2 selected four adjacent strips with a length of 50 m and width of 2.2 m in the main and secondary rockfill zones, respectively. Each test strip was divided into ten small test areas with the grid of 5 m long and 2.2 m wide and numbered ①–⑩, as shown in Figure 7. The area with odd number is the buffer area in the rolling process, and we take the test data on the even-numbered area for analysis. When the required rolling process (Figure 7) for each strip is finished, the digging test method is used to obtain the conventional compaction quality indexes in the even-numbered areas.

4. Results and Discussion

This section focuses on analyzing the correlations among rolling parameters, real-time test indexes, and compaction quality indexes according to the dataset from the two-part experiment described above. In the analysis of data correlation, the linear model and hyperbolic model are compared in a bid to determine the correlation degree of the data and establish a more appropriate correlation formula. In addition, the spectrum analysis and discussion is conducted to make an in-depth analysis on the frequency distribution regularity of acceleration signal and compare the test effects of the four indexes on different test materials.

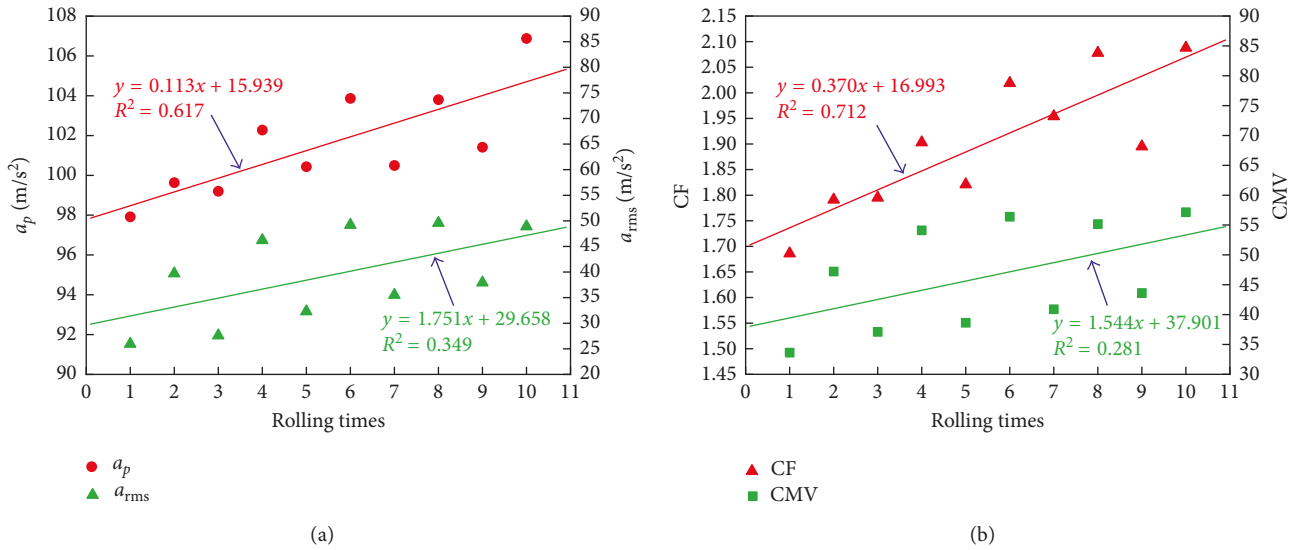


FIGURE 8: Linear relationships between real-time test indexes and rolling times. (a) a_p , a_{rms} . (b) CF, CMV.

4.1. Result Analysis of Experiment Part 1

4.1.1. *Correlations between Rolling Times and the Four Indexes.* A total of 360 groups of valid data were obtained in the experiment of change in rolling times. The scatter diagram of the indexes measured on each small test area was plotted with the Origin software so as to analyze the correlation between the real-time test indexes and rolling times.

The linear model is commonly used for the correlation analysis in the study field [30–33], and the function expression of which is

$$y = a + bx, \quad (10)$$

where a and b are the regression coefficients.

Firstly, the linear model was used in the regression analysis, and the result of a certain area on the main rockfill is shown in Figure 8.

From the scatter diagram, the following two characteristics are identified:

- (1) The variable y increases with the rise of x , but its growth rate gradually slows down.
- (2) When variable x increases further, y gradually comes to a constant, which indicates that the curve may have a horizontal asymptote.

Thus, it can be assumed that the trend line of the scatter plot is a hyperbolic curve and the function formula of which can be expressed as

$$y = \frac{x}{ax + b}, \quad (11)$$

where a and b are the regression coefficients.

Then, the hyperbolic model was used to analyze the scatter plot described above, and the result is shown in Figure 9.

The determination coefficients (R^2) of the regression models on the small test areas of each strip are evaluated

using the trimmed mean to reduce the effect of an accidental error. The results are shown in Table 2. From this table, it can be seen that there are some correlations between all the four test indexes and rolling times on each tested dam material. Specifically, the linear correlation between CF and rolling times is the strongest, with all the determination coefficients (R^2) being over 0.7.

When considering the practical application of a test index, both its correlation degree and stability of the data in different test areas need to be taken into account. Therefore, the standard deviation coefficients (V_σ) of the 120 groups of data measured on each testing material were calculated to analyze the discrete degree of the dataset. It can be seen from the results (Table 3) that with the increase of the particle size in the filter material, the secondary rockfill and main rockfill, the V_σ of each test index also gradually increase, while the V_σ of a_p , a_{rms} , and CF stay at a low level, indicating that the data stability of a_p , a_{rms} , and CF is better.

4.1.2. *Correlations between Running Speed, Compaction Thickness, and the Four Indexes.* In the experiment of change in running speed and compaction thickness, 24 sets of valid data were obtained on the main and secondary rockfill, respectively. The changes of real-time indexes brought by the two parameters on secondary rockfill are shown in Figures 10 and 11, respectively.

It can be inferred from Figures 11 and 12 that the a_p and CF show a significant downward trend with the increase of running speed and compaction thickness, respectively, and the two indexes increase regularly with the growth of rolling times. Though a_{rms} and CMV rise along with the number of rolling times in Figure 11(b), they do not show the tendency in Figure 12(b). And there is no obvious regularity in the tendencies of a_{rms} and CMV when the roller running speed and soil compaction thickness change. The results of the test on the main rockfill are the same as

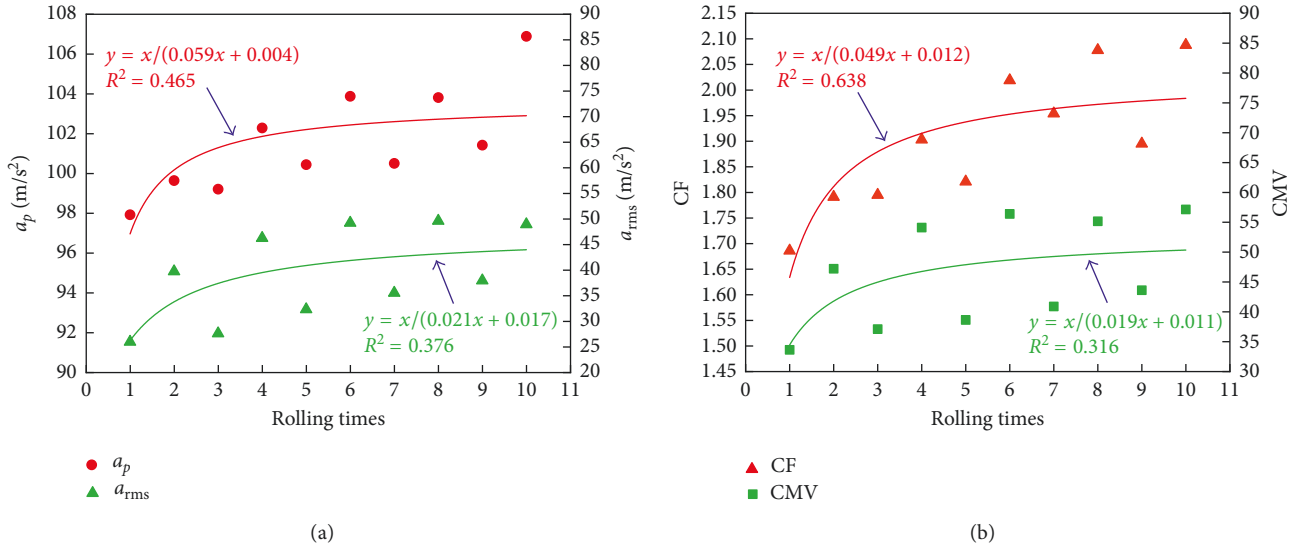


FIGURE 9: Hyperbolic relationships between real-time test indexes and rolling times. (a) a_p , a_{rms} . (b) CF, CMV.

TABLE 2: Determination coefficients (R^2) for regression analysis between real-time test indexes and rolling times.

Testing material	a_p		a_{rms}		CF		CMV	
	Linear model	Hyperbolic model	Linear model	Hyperbolic model	Linear model	Hyperbolic model	Linear model	Hyperbolic model
Main rockfill	0.601	0.628	0.584	0.486	0.731	0.679	0.496	0.498
Secondary rockfill	0.663	0.687	0.595	0.523	0.784	0.721	0.535	0.579
Filter material	0.672	0.704	0.630	0.572	0.796	0.752	0.670	0.604

TABLE 3: Standard deviation coefficients (V_σ) of real-time test indexes (%).

Testing material	a_p	a_{rms}	CF	CMV
Main rockfill	5.61	4.35	2.44	14.27
Secondary rockfill	2.90	2.88	1.27	13.28
Filter material	2.15	1.59	1.03	10.03

those on the secondary rockfill, which will not be repeated hereby.

For energy-related analysis, when the roller running speed and soil compaction thickness increase, the energy absorbed by the soil in unit and volume will decrease, respectively. With the same rolling times, the soil compaction degree is reduced. The same goes to the reaction force of the soil to the vibratory roller, which results in a decrease of the roller vibratory acceleration. Therefore, all the four derived indexes should show a declining trend, and only the tendency of a_p and CF among them are consistent with the theoretical situation.

4.2. Result Analysis of Experiment Part 2. Experiment part 2 obtained twenty groups of real-time test index and compaction quality index data on the main and secondary rockfill, respectively. For the main and secondary rockfill in the project, the main compaction quality control indexes

are porosity (P) and relative density (D_r), respectively [36]. The correlation analysis of real-time test indexes and the two compaction quality indexes is conducted in this section.

The linear regression model and hyperbolic regression model were utilized to analyze the scatter diagram plotted by the Origin software. The results of linear regression analysis on the main rockfill are shown in Figure 12, and the results on the secondary rockfill are shown in Figure 13. The determination coefficients (R^2) of the regression models are shown in Table 4.

As can be seen from Table 4, in the correlation analysis of the four test indexes and porosity, the hyperbolic model of CF and the index shows the highest R^2 of 0.823. As for relative density, the linear model of CF and the index registers the highest R^2 of 0.820. This means that the correlation between CF and the compaction quality indexes is the strongest among the four test indexes, and the regression functions can be expressed as

$$CF = \frac{P}{0.802P - 6.430}, \quad (12)$$

$$CF = 0.284D_r + 1.725. \quad (13)$$

The compaction quality control criteria on the main and secondary rockfill are $P \leq 21\%$ and $D_r \geq 0.90$, respectively. The criterion of $CF \geq 2.017$ can be got by taking $P \leq 21\%$ into (12), and $CF \geq 1.981$ can be obtained by plugging $D_r \geq 0.90$

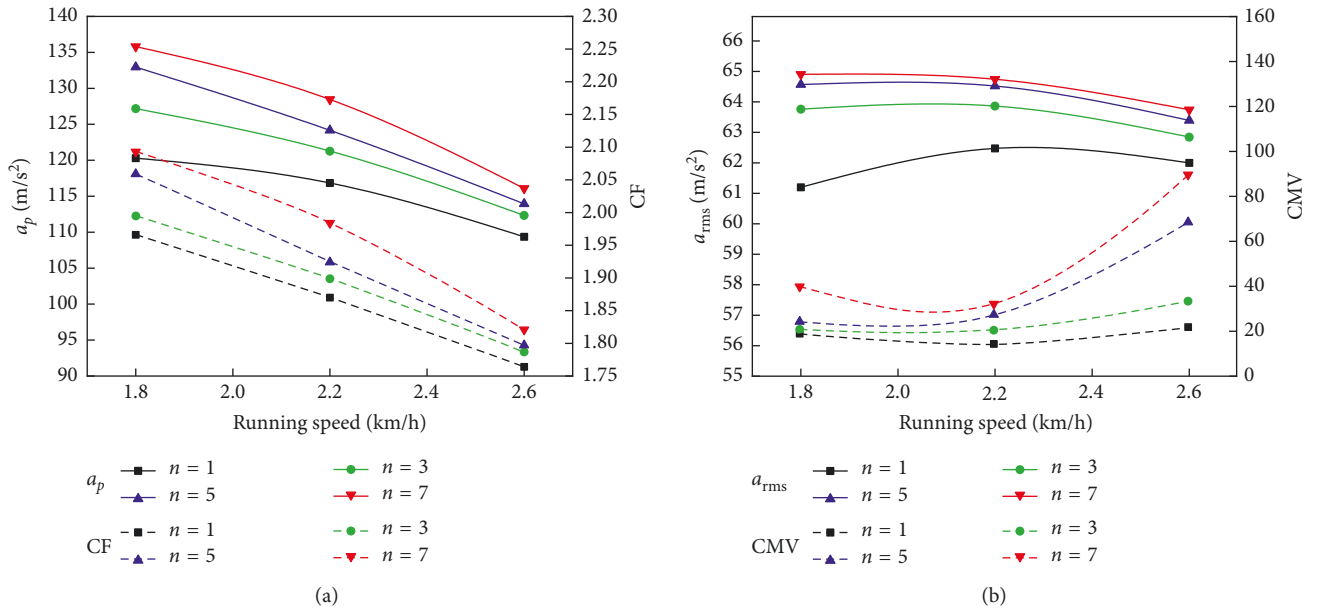


FIGURE 10: Tendency of real-time indexes with the change of running speed. (a) a_p , CF. (b) a_{rms} , CMV.

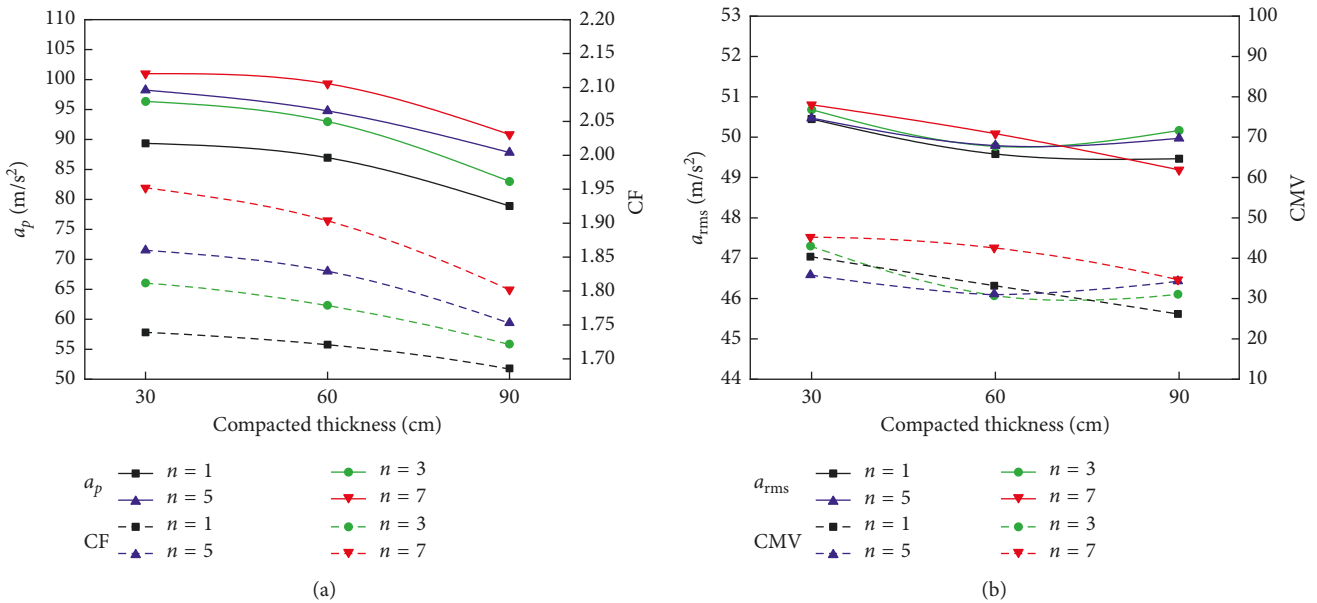


FIGURE 11: Tendency of real-time indexes with the change of compaction thickness. (a) a_p , CF. (b) a_{rms} , CMV.

into (13). It is thus tentatively believed that the compacted soil achieves the required compaction quality when the CF values reach 2.017 and 1.981 on the main and secondary rockfills, respectively. The more precise control criteria of CF values need to be determined based on the quantitative relations among the soil compaction degree, the reaction force of the soil (characterized by the acceleration indexes discussed in the paper), and the strength and stiffness of the rockfill material, which will be studied in the future work.

4.3. *Spectrum Analysis and Discussion.* In order to analyze the application scope of the four indexes, this section conducted a spectrum analysis of the acceleration signal and had a further discussion about the test effects of the four indexes on different test materials. Figures 14–16 show the comparison of the acceleration signal and indexes in the eighth compaction pass of the main rockfill and filter material. The 3D spectra in Figure 15 are obtained through the fast Fourier transformation (FFT) analysis of the

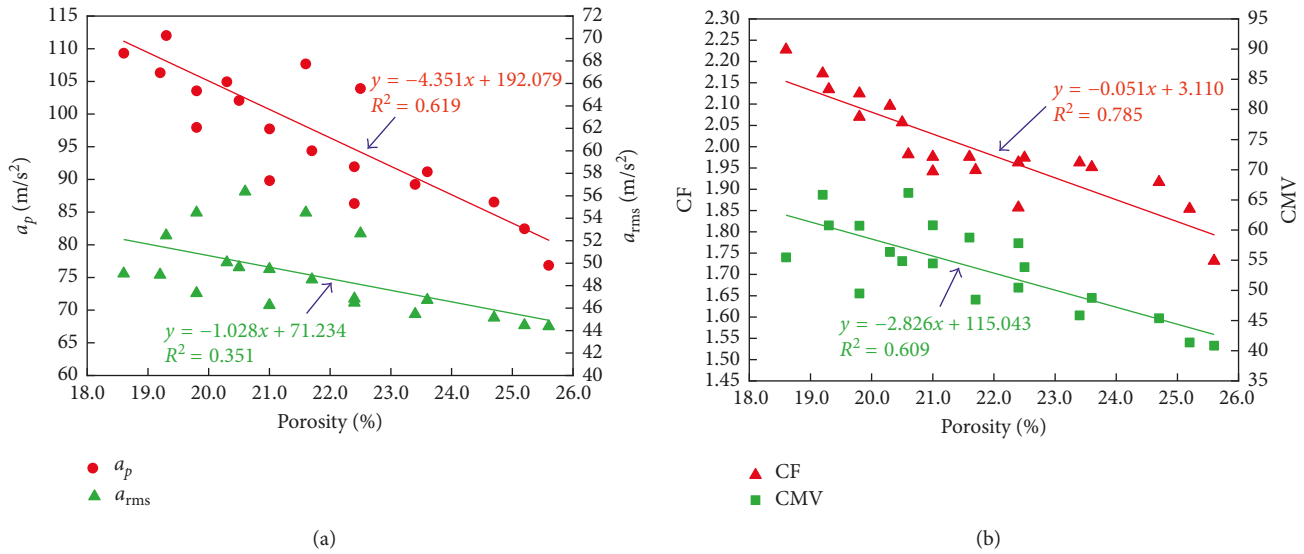


FIGURE 12: Linear relationships between porosity and real-time indexes on the main rockfill. (a) a_p , a_{rms} . (b) CF, CMV.

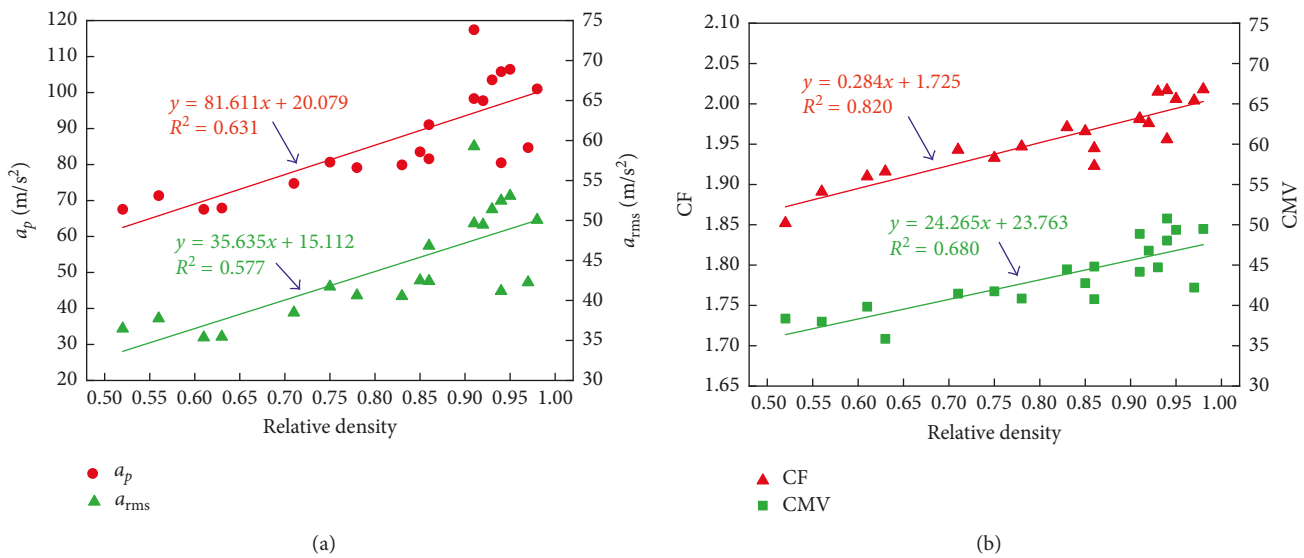


FIGURE 13: Linear relationships between relative density and real-time indexes on the secondary rockfill. (a) a_p , a_{rms} . (b) CF, CMV.

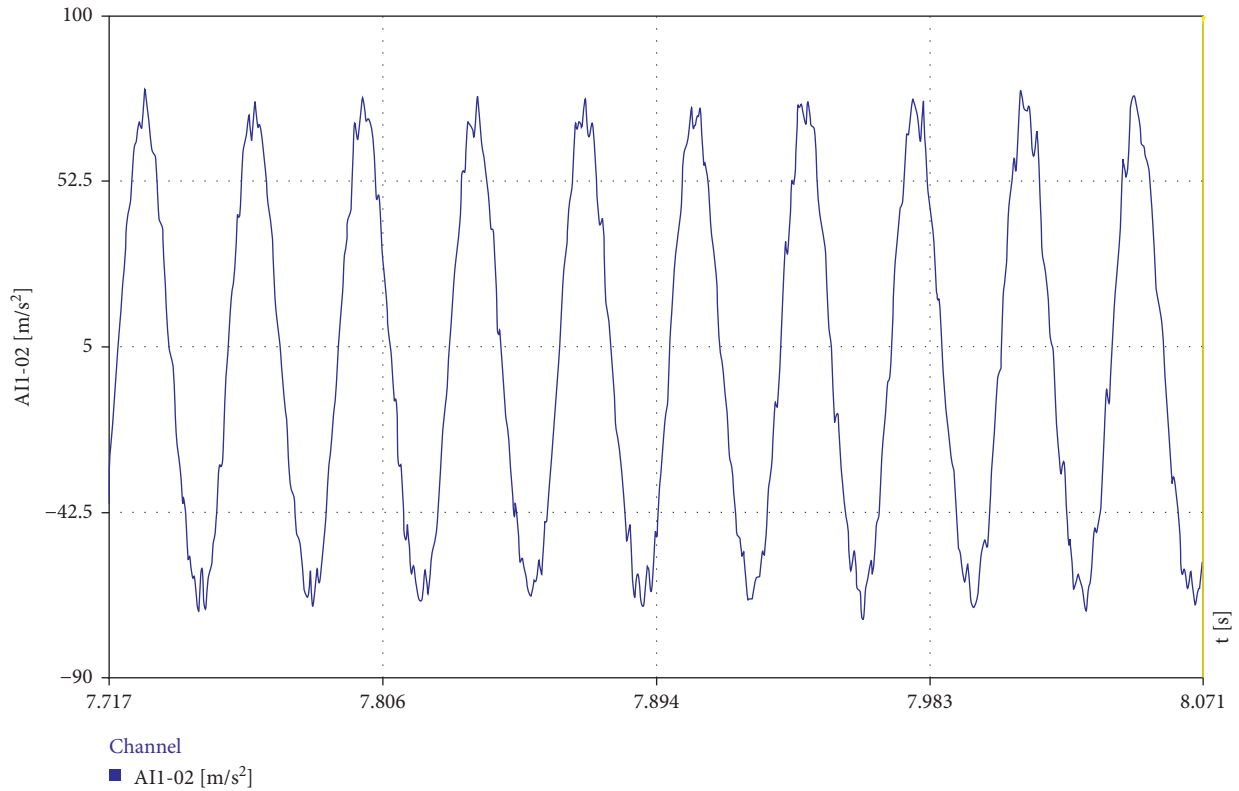
TABLE 4: Determination coefficients (R^2) for regression analysis between real-time test indexes and compaction quality indexes.

Compaction quality index	a_p		a_{rms}		CF		CMV	
	Linear model	Hyperbolic model	Linear model	Hyperbolic model	Linear model	Hyperbolic model	Linear model	Hyperbolic model
Porosity	0.619	0.580	0.351	0.308	0.785	0.823	0.609	0.528
Relative density	0.631	0.622	0.577	0.564	0.820	0.804	0.680	0.650

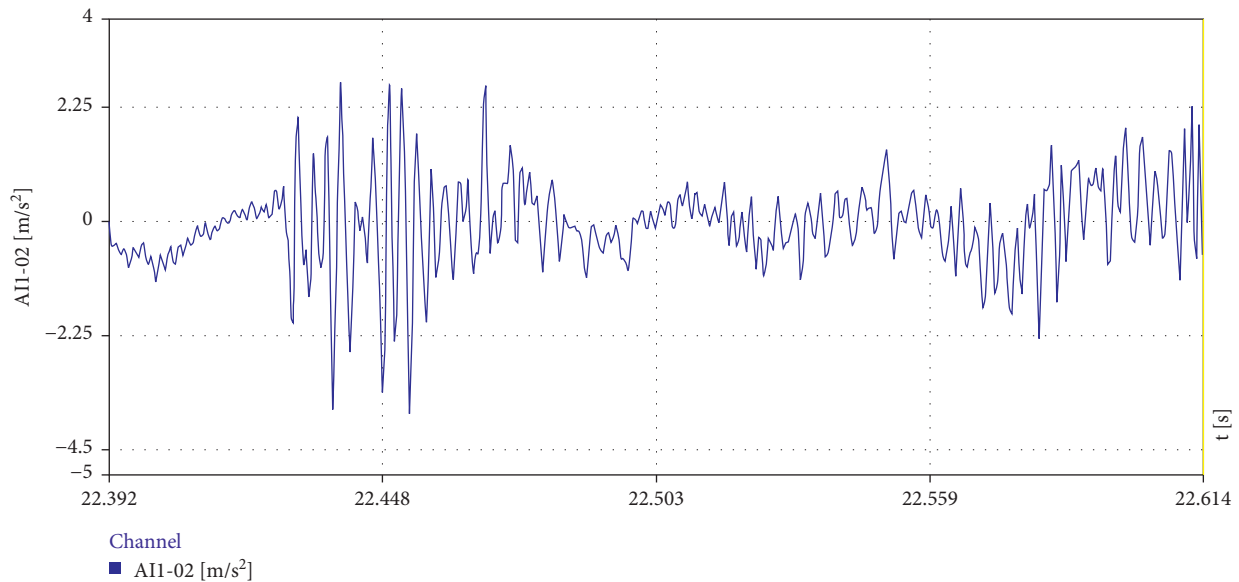
acceleration signal. The CF value in Figure 16 is magnified tenfold to display its tendency clearly.

As can be seen from Figure 14, the acceleration waveform is regularly distorted when the filter material get compacted, while the acceleration wave changes chaotically on the main rockfill. The spectra of Figure 15 show that the frequencies of the acceleration signal on

the filter material are regularly distributed with stable fundamental frequency, first and second harmonic components, and few higher frequency components in the rolling process. While the spectrum on the main rockfill shows that the frequency distribution of the acceleration signal is irregular and disorderly with unsystematic frequency components.



(a)



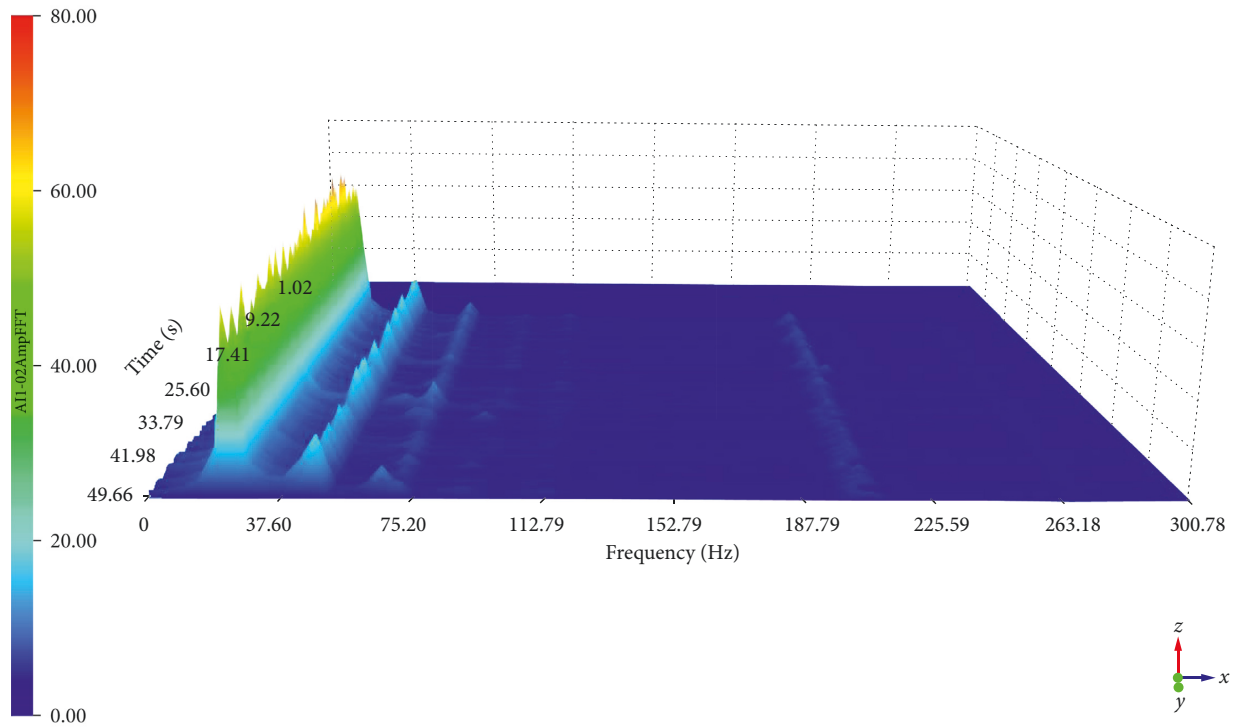
(b)

FIGURE 14: Time-history curve of acceleration signal. (a) Filter material. (b) Main rockfill.

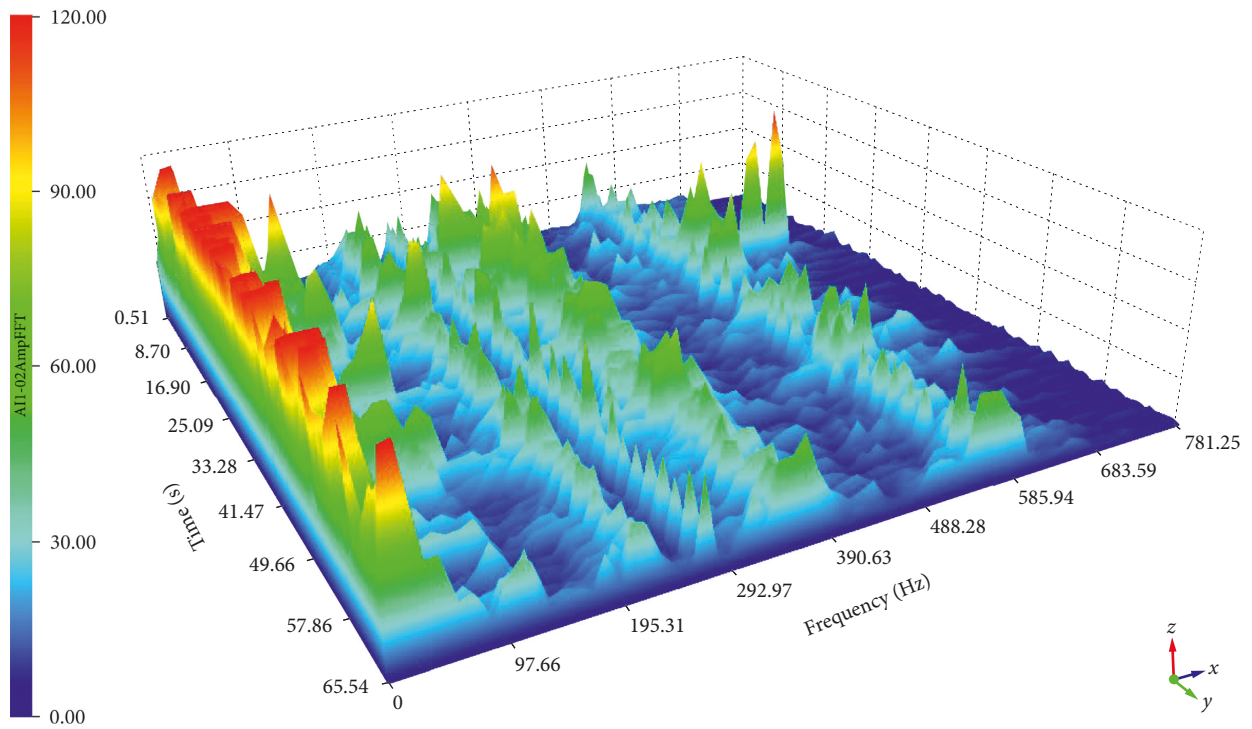
Analysis of the reasons shows that since the main contents of the filter material are spherical particles with few edges, the contact between the soil particles and roller is relatively even, and there is not much difference among the reaction forces of the soil to the roller in unit areas. With the rolling moving on, the soil becomes more compacted and the reaction force to the roller increases, which causes a regular increase in the

amplitude of the harmonic components and a regular wave distortion of the acceleration signal. Therefore, CMV and other acceleration indexes have a regular change in the rolling process, and all the four indexes can well reflect the compaction degree of the fine-grained soil.

However, in the case of the rockfill material which contains many sharp-edged stones, the contact between the



(a)



(b)

FIGURE 15: Three-dimensional spectra of acceleration signal. (a) Filter material. (b) Main rockfill.

soil particles and the roller is uneven, resulting in significant differences among the reaction forces of the soil to the roller in unit areas. The energy in the reaction force of the soil is unevenly transmitted to the roller, which leads to an

irregular frequency distribution and a clutter waveform of the acceleration signal on the rockfill material. Due to the unstable change of the amplitude of fundamental frequency and first harmonic component in the rolling process, CMV

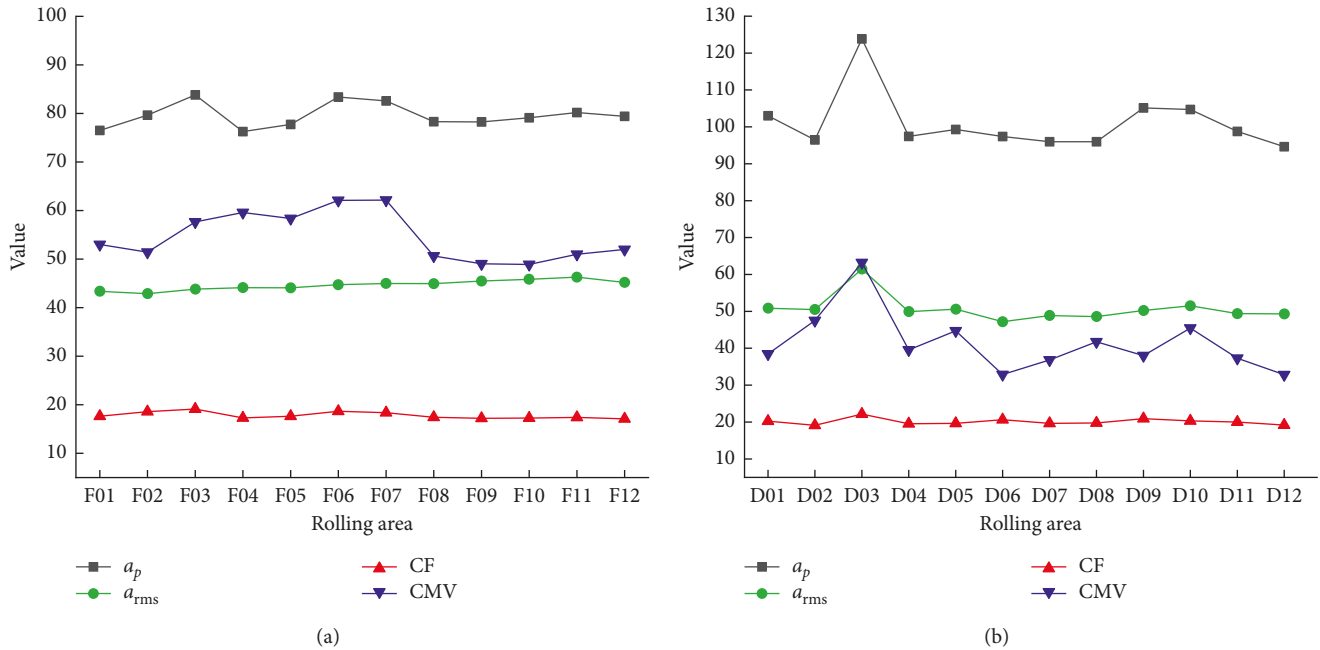


FIGURE 16: Tendency of acceleration indexes in the eighth compaction pass. (a) Filter material. (b) Main rockfill.

is disadvantaged in characterizing the compaction degree of the rockfill.

Judging from the physical meaning, the a_p and a_{rms} can only reflect part of the characteristics of the acceleration signal, while the CF combines the variation trend of them and describes the ability of the soil to produce the greatest reaction force to the roller. Therefore, the effect of the unevenness of the dam material on CF is relatively small compared to a_p and a_{rms} , which is consistent with the test result that the V_σ of CF is smaller than that of a_p and a_{rms} on all test materials (Table 3). The result can be proved by Figure 16 that the CF value changes stably while other indexes have greater volatility in the rolling process of the same dam material.

Combined with the analyses above, it can be known that the CF index best characterizes the compaction degree of the rockfill material among the four indexes. In the future, the authors will further establish a more detailed vibration model from the theoretical perspective, derive the formula, and clearly distinguish the applicability of CF index and other three acceleration indexes on the rockfill material.

5. Conclusions

In this study, the authors utilized four derived acceleration indexes to characterize the soil compaction degree, including a_p , a_{rms} , CF, and CMV. A two-part field compaction test was performed to analyze and judge the test effects of the four indexes on the rockfill and other dam materials. After the data correlation analysis and signal spectrum analysis, the following conclusions can be drawn:

- (1) The data of a_p , a_{rms} , and CF are stable with low V_σ of them, and only the tendencies of a_p and CF with the change of roller running speed and compacted soil thickness are consistent with the theoretical situation. Besides, the linear correlation between CF and rolling times is the strongest, with the trimmed mean of R^2 being over 0.7 on all test materials. Thus, the correlation between CF and the rolling parameters is the strongest among the four indexes.
- (2) The correlation between CF and the two compaction quality indexes is the strongest among the four indexes, with the highest R^2 of 0.823 and 0.820 in the regression analysis, respectively. The tentative control criteria of $CF \geq 2.017$ on the main rockfill and $CF \geq 1.981$ on the secondary rockfill are given by establishing the quantitative relations between CF and compaction quality indexes, which can instruct the field compaction quality control in the rolling process.
- (3) The signal spectrum analysis shows that the frequencies of the acceleration signal on filter material are regularly distributed, and all the four indexes can well reflect the compaction degree of the fine-grained soil. The frequency distribution of the acceleration signal on main rockfill is irregular, and CMV is disadvantaged in characterizing the compaction degree of the rockfill. The effect of the unevenness of the dam material on CF is relatively small compared to a_p and a_{rms} . Combined with the results of statistical regression analyses, it can be concluded that the CF index best characterizes the compaction

degree of the rockfill material among the four indexes.

Conflicts of Interest

The authors declare that they have no conflicts of interest.

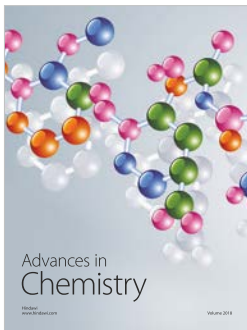
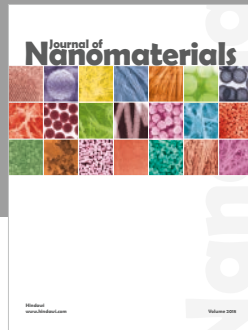
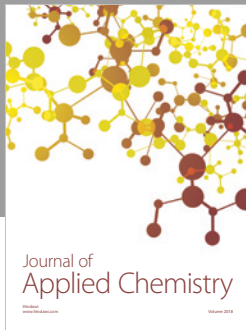
Acknowledgments

The authors wish to thank the great help of Sinohydro Bureau 5 Co., Ltd., in the field test. This work was supported by the National Science and Technology Support Program of China (no. 2014BAB03B04), the Research Foundation for Young Teachers of Sichuan University (no. 2016SCU11039), and the Science and Technology Program of the Power Construction Corporation of China (no. ZDZX-05).

References

- [1] Trade Standard of P. R. China, "Specifications for rolled earth-rockfill dam construction," Tech. Rep. DL/T 5129-2013, National Energy Administration of P. R. China, Beijing, China, 2013.
- [2] H. Thurner and A. Sandstrom, "A new device for instant compaction control," in *Proceedings of the International Conference on Compaction*, vol. 2, pp. 611-614, Paris, France, 1980.
- [3] A. Sandstrom and J. C. Pettersson, "Intelligent systems for QA/QC in soil compaction," in *Proceedings of the 83rd Annual Transportation Research Board Meeting, Transportation Research Board*, pp. 1-17, Washington, DC, USA, 2004.
- [4] D. Adam, "Continuous compaction control (CCC) with vibratory rollers," in *Proceedings of the 1st Australia-Newzealand Conference on Environmental Geotechnics-GeoEnvironment*, pp. 245-250, Melbourne, VIC, Australia, 1997.
- [5] H. Brandl and D. Adam, "Sophisticated continuous compaction control of soils and granular materials," in *Proceedings of the 14th International Conference on Soil Mechanics and Foundation Engineering*, pp. 1-6, Hamburg, Germany, 1997.
- [6] D. J. White, "Report of the workshop on intelligent compaction for soils and HMA," in *Proceedings of the Workshop on Intelligent Compaction for Soils and HMA*, pp. 1-129, Des Moines, IA, USA, April 2008.
- [7] G. Chang, Q. W. Xu, J. Rutledge et al., *Accelerated Implementation of Intelligent Compaction Technology for Embankment Subgrade Soils, Aggregate Base, and Asphalt Pavement Materials*, Federal Highway Administration, Washington, DC, USA, 2011.
- [8] L. Forssblad, "Compaction meter on vibrating rollers for improved compaction control," in *Proceedings of the International Conference on Compaction*, vol. 2, pp. 541-546, Paris, France, 1980.
- [9] L. Forssblad, *Vibratory Soil and Rock Fill Compaction*, Swedish National Road and Transport Research Institute (VTI), Dynapac Maskin, Karlskrona, Sweden, 1981.
- [10] L. Forssblad, "Roller-Mounted compaction meters," in *Proceedings of the 10th International Road Federation*, pp. 1-8, RJ, Brazil, 1984.
- [11] L. Forssblad, "Soil compaction and compaction control," in *Proceedings of the 3rd International Geotechnical Seminar*, pp. 1-8, Singapore, 1985.
- [12] H. Fujii, "Comparison of various control methods in situ," in *Proceedings of the 1st Asian-Pacific Conference of International Society Terrain-Vehicle Systems*, pp. 10-18, Beijing, China, 1986.
- [13] X. L. Guo and D. Wen, *Field Compaction of Coarse Aggregates*, China Water & Power Press, Beijing, China, (Chinese), 1999.
- [14] G. Komandi, "An evaluation of the concept of rolling resistance," *Journal of Terramechanics*, vol. 36, no. 3, pp. 159-166, 1999.
- [15] D. J. White, T. D. Rupnow, and H. Ceylan, "Influence of subgrade/subbase non-uniformity on PCC pavement performance," in *Proceedings of the Geotechnical Engineering for Transportation Projects (GeoTrans2004)*, pp. 1058-1065, ASCE, Los Angeles, CA, USA, July 2004.
- [16] M. G. Bekker, *Introduction to Terrain-Vehicle Systems*, University of Michigan Press, Ann Arbor, MI, USA, 1969.
- [17] M. J. Thompson and D. J. White, "Field calibration and spatial analysis of compaction-monitoring technology measurements," *Transportation Research Record: Journal of the Transportation Research Board*, vol. 2004, pp. 69-79, 2007.
- [18] M. J. Thompson and D. J. White, "Estimating compaction of cohesive soils from machine drive power," *Journal of Geotechnical and Geoenvironmental Engineering*, vol. 134, no. 12, pp. 1771-1777, 2008.
- [19] D. J. White and M. J. Thompson, "Relationships between in situ and roller-integrated compaction measurements for granular soils," *Journal of Geotechnical and Geoenvironmental Engineering*, vol. 134, no. 12, pp. 1763-1770, 2008.
- [20] W. Krober, R. Floss, and W. Wallrath, "Dynamic soil stiffness as quality criterion for soil compaction," *Geotechnics for Roads, Rail Tracks and Earth Structures*, pp. 189-199, Balkema, Rotterdam, Netherlands, 2001.
- [21] M. A. Mooney and R. V. Rinehart, "Field monitoring of roller vibration during compaction of subgrade soil," *Journal of Geotechnical and Geoenvironmental Engineering*, vol. 133, no. 3, pp. 257-265, 2007.
- [22] R. V. Rinehart and M. A. Mooney, "Instrumentation of a roller compactor to monitor vibration behavior during earthwork compaction," *Automation in Construction*, vol. 17, no. 2, pp. 144-150, 2008.
- [23] R. Anderegg and K. Kaufmann, "Intelligent compaction with vibratory rollers: feedback control systems in automatic compaction and compaction control," *Transportation Research Record: Journal of the Transportation Research Board*, vol. 1868, pp. 124-134, 2004.
- [24] R. Anderegg, D. A. von Felten, and K. Kaufmann, "Compaction monitoring using intelligent soil compactors," in *Proceedings of the Geotechnical Engineering in the Information Technology Age (GeoCongress2006)*, pp. 41-46, ASCE, Atlanta, GA, USA, April 2006.
- [25] K. Kaufmann and R. Anderegg, "3D-construction applications III: GPS-based compaction technology," in *Proceedings of the 1st International Conference on Machine Control & Guidance*, pp. 1-10, Zurich, Switzerland, 2008.
- [26] G. H. Xu and Y. Cai, "Dynamics monitor in the process of road structure forming," in *Proceedings of the 15th International Road Federation (IRF) World Meeting*, Thailand, 2005.
- [27] T. S. Yoo, *A Theory for Vibratory Compaction of Soil*, pp. 44-52, State University of New York at Buffalo, New York, NY, USA, 1975.
- [28] E. T. Selig and T. S. Yoo, "Fundamentals of vibratory roller behavior," in *Proceedings of the 9th International Conference*

- on *Soil Mechanics and Foundation Engineering*, pp. 375–380, Tokyo, Japan, 1977.
- [29] T. S. Yoo and E. T. Selig, “Dynamics of vibratory-roller compaction,” *Journal of the Geotechnical Engineering Division*, vol. 105, no. 10, pp. 1211–1231, 1979.
- [30] D. H. Zhong, B. Cui, D. H. Liu, and D. Tong, “Theoretical research on construction quality real-time monitoring and system integration of core rock-fill dam,” *Science in China Series E: Technological Sciences*, vol. 52, no. 11, pp. 3406–3412, 2009.
- [31] D. H. Zhong, D. H. Liu, and B. Cui, “Real-time compaction quality monitoring of high core rockfill dam,” *Science China Technological Sciences*, vol. 54, no. 7, pp. 1906–1913, 2011.
- [32] D. Liu, J. Sun, D. Zhong, and L. Song, “Compaction quality control of earth-rock dam construction using real-time field operation data,” *Journal of Construction Engineering and Management*, vol. 138, no. 9, pp. 1085–1094, 2012.
- [33] D. Liu, Z. Li, and Z. Lian, “Compaction quality assessment of earth-rock dam materials using roller-integrated compaction monitoring technology,” *Automation in Construction*, vol. 44, pp. 234–246, 2014.
- [34] R. B. W. Heng and M. J. M. Nor, “Statistical analysis of sound and vibration signals for monitoring rolling element bearing condition,” *Applied Acoustics*, vol. 53, no. 1-3, pp. 211–226, 1998.
- [35] Trade Standard of P. R. China, “Specification of soil test,” Tech. Rep. SL237–1999, Ministry of Water Resources of P. R. China, Beijing, China, 1999.
- [36] Trade Standard of P. R. China, “Specification on rockfill dam built with gravel and soil core wall in hydroelectric and hydraulic engineering,” Tech. Rep. DL/T 5269–2012, National Energy Administration of P. R. China, Beijing, China, 2012.



Hindawi
Submit your manuscripts at
www.hindawi.com

